MAGNETIC FIELD MEASUREMENT

RELEVANCE OF ELECTROMAGNETIC FIELD MEASUREMENTS

The measurement of electromagnetic (em) fields is relevant for various purposes: for scientific and technical applications, for radio propagation, for Electromagnetic Compatibility (EMC) tests (i.e. testing of the immunity of electronic equipment to electromagnetic fields and the measurement of radiated electromagnetic emissions aiming at the protection of radio reception from radio interference), and for safety reasons (i.e. the protection of persons from excessive field strengths). For radio propagation and EMC measurements, below about 30 MHz a distinction is made between electric and magnetic components of the em field to be measured. In the area of human safety, this distinction is continued to even higher frequencies.

QUANTITIES AND UNITS OF MAGNETIC FIELDS

Especially in the measurement of radio propagation and of radio interference, magnetic field measurements with loop antennas have traditionally been used to determine the received field intensity which was quantified in units of the electric field strength, i.e. in μV/m, respectively, in dB(μV/m). For radio propagation this can be justified for far field conditions where electric field strength E and magnetic field strength H are related via the impedance Z_0 of the free space; $E = HZ_0$ (see also antenna factor definition). Commercial EMC standards (1) and (2) specify radiated disturbance measurements below 30 MHz with a loop antenna; however, until 1990 measurement results and limits were expressed in dB(μV/m). Since this measurement is done at less than the far field distance from the equipment under test (EUT) over a wide frequency range, the use of units of the electric field strength was difficult to justify. Therefore, the CISPR (the International Special Committee on Radio Interference) decided in 1990 to use units of the magnetic field strength μA/m, respectively, dB(μA/m).

Guidelines and standards for human exposure to em fields specify the limits of electric and magnetic fields. In the low frequency range [i.e., below 1 MHz (3)], limits of the electric field strength are not proportional to limits of the magnetic field strength. Magnetic field limits in frequency ranges below 10 kHz are frequently expressed in units (T and G, for Tesla and Gauss) of the magnetic flux density B despite the absence of magnetic material in human tissue. Some standards specify magnetic field limits in A/m instead of T (see (4) in contrast to (5)). For easier comparison with other applications we therefore convert limits of the magnetic flux density to limits of the magnetic field strength using $H = B/\mu_0$ or 1 T = $10^7/4\pi$ A/m $\approx 0.796 \cdot 10^6$ A/m and 1 G = 79.6 A/m. At higher frequency ranges all standards specify limits of the magnetic field strength in A/m. Above 1 MHz the limits of the magnetic field strength are related to limits of the electric field strength via the impedance of the free space. Nevertheless both quantities, electric and magnetic fields, have to be measured, since in the near field the exposition to either magnetic or electric field may be dangerous.

RANGE OF MAGNETIC FIELD LEVELS TO BE CONSIDERED FOR MEASUREMENT

In order to show the extremely wide range of magnetic field levels to be measured, we give limits of some national or regional standards. In different frequency ranges and applications magnetic field strength limits vary from as much as 10 MA/m down to less than 1 nA/m (i.e. over 16 decades). This wide range of field-strength levels will normally not be covered by one magnetic field meter. Different applications require either broadband or narrowband equipment.

On the high level end there are safety levels and limits of the magnetic field strength for the protection of persons which vary from as much as 4 MA/m (i.e. 4×10^6 A/m corresponding to the specified magnetic flux density of 5 T in nonferrous material) at frequencies below 0.1 Hz, to less than 0.1 A/m at frequencies above 10 MHz (see Fig. 1) (3–6). These limits of the magnetic field strength are derived from basic limits of the induced body current density (up to 10 MHz), respec-

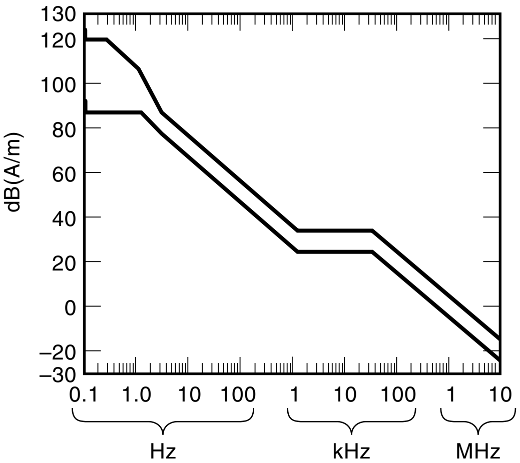

Figure 1. Safety limits of the magnetic field strength derived from the European Prestandard ENV 50166 Parts 1 and 2: 120 dB(A/m) are equivalent to 1 MA/m corresponding to 1.25 T, 0 dB(A/m) are equivalent to 1 A/m.

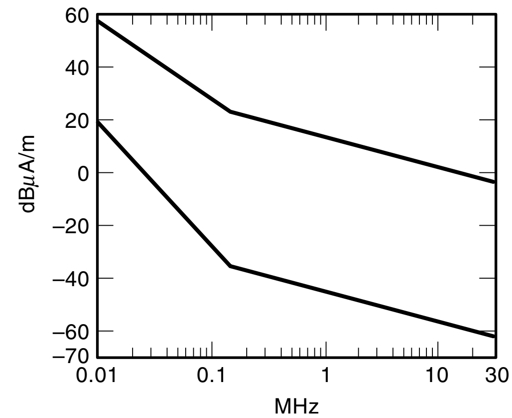

Figure 3. Narrowband emission limits of the magnetic field strength derived from the German military standard VG 95343 Part 22 (8). This standard gives the limits of $H \cdot Z_0$ in dB(μV/m) of four equipment classes, the emissions have to be measured with a loop antenna calibrated in dB(μV/m) in the near field of the equipment under test (EUT). Therefore, the limits have been converted into dB(μA/m). The lower limit is Class 1, the upper is Class 4.

tively, basic limits of the specific absorption rate (SAR, above 10 MHz). There are also derived limits of the electric field strength which are however not of concern here.

By using an approach different from the one of the safety standards, the Swedish standard MPR II, which has become an international de-facto standard for video display units (VDU) without scientific proof, specifies limits of the magnetic flux density in two frequency ranges, which are bounded by filters: a limit of 40 nT ($\approx$0.032 A/m) in the range 5 Hz to 2 kHz and a limit of 5 nT ($\approx$0.004 A/m) in the range 2 kHz to 400 kHz.

On the low level end there are limits for the protection of radio reception and electromagnetic compatibility in some military standards (see Figs. 2 and 3).

International and national monitoring of radio signals and the measurement of propagation characteristics require the measurement of low-level magnetic fields down to the order of -30 dB(μA/m): see also subsequent discussions and refs. 7–9. For the protection of radio reception, international, regional (e.g. European) and national radiated emission limits and measurement procedures have been standardized for industrial, scientific, medical (ISM) and other equipment (1,2,10–12). An example is given in Fig. 4.

Radiated emission limits of fluorescent lamps and luminaires are specified in a dB(μA) using a large-loop-antenna system (LAS) (10). For further information, see the text below.

EQUIPMENT FOR MAGNETIC FIELD MEASUREMENTS

Magnetic Field Sensors Other Than Loop Antennas

An excellent overview of magnetic field sensors other than loop antennas is given in Ref. 13. Table 1 lists the different

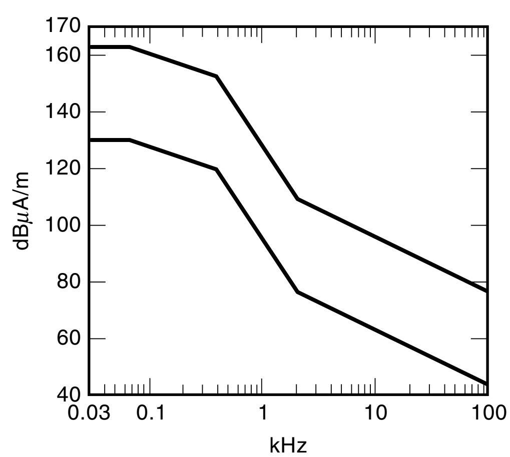

Figure 2. Magnetic field strength limits derived from US MIL-STD-461D RE101 (Navy only) (7). These limits are originally given in dB(pT) (decibels above 1 pT). The measurement procedure requires a 36 turn shielded loop antenna with a diameter of 13.3 cm. Measurement distance is 7 cm for the upper limit and 50 cm for the lower limit.

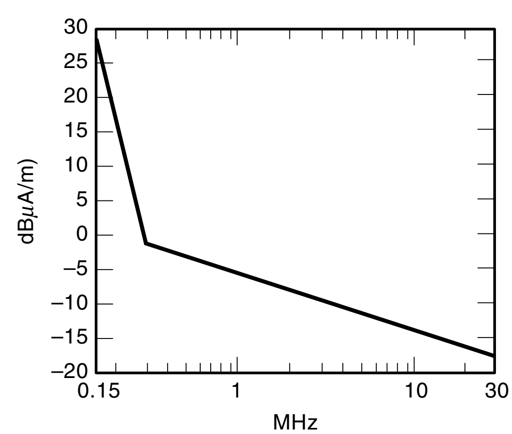

Figure 4. Radiated emission limits for navigational receivers according to draft revision IEC 945 (IEC 80/124/FDIS), originally given in dB(μV/m), for the purpose of this article converted into dB(μA/m).

Table 1. Overview over Different Magnetic Field Sensors, their Underlying Physical Effects, their Applicable Level, and Frequency Ranges from Ref. 73. For Easier Comparison with the Rest of the Text, the Values of Ref. 73 Have Been Converted from G into A/m

Type	Principle of Operation	Level of Operation	Frequency Range
Search-coil magnetometer	Faraday's law of induction	10^{-6} to 10^{9} A/m	1 Hz to 1 MHz
Flux-gate magnetometer	Induction law with hysteresis of magnetic material	10^{-4} to 10^{4} A/m	dc to 10 kHz
Optically pumped magnetometer	Zeeman effect: splitting of spectral lines of atoms	10^{-6} to 10^{2} A/m	dc
Nuclear-precession magnetometer	Response of nuclei of atoms to a magnetic field	10^{-5} to 10^{2} A/m	dc (upper frequency limited by gating frequency of hydrocarbon fluid)
SQUID magnetometer	Superconducting quantum interference device	10^{-8} to 10^{-2} A/m; speciality: differential field measurements	dc
Hall-effect sensor	Hall effect	10^{-1} to 10^{5} A/m	dc to 1 MHz
Magnetoresistive magnetometer	Magnetoresistive effect	10^{-4} to 10^{4} A/m	dc to 1 GHz
Magnetodiode	Semiconductor diode with undoped silicon	10^{-2} to 10^{3} A/m	dc to 1 MHz
Magnetotransistor	Hall and Suhl effects	10^{-3} to 10^{3} A/m	dc to 1 MHz
Fiberoptic magnetometer	Mach–Zehnder interferometer	10^{-7} to 10^{3} A/m	dc to 60 kHz
Magnetooptical sensor	Faraday polarization effect	10^{2} to 10^{9} A/m	dc to 1 GHz

types of field sensors which are exploiting different physical principles of operation.

Magnetic Field-Strength Meters With Loop Antennas

Especially for the measurement of radio wave propagation and radiated electromagnetic disturbance pick-up devices, the antennas become larger and therefore they are used separate from the indicating instrument (see Fig. 5). The instrument is a selective voltmeter, a measuring receiver or a spectrum analyzer. The sensitivity pattern of a loop antenna can be represented by the surface of two spheres (see Figs. 6 and 7). In order to determine the maximum field strength, the loop antenna has to be turned into the direction of maximum sensitivity.

To obtain an isotropic field sensor, three loops have to be combined in such a way that the three orthogonal components of the magnetic field H_x, H_y and H_z are combined to fulfill the equation

$$H = \sqrt{H_x^2 + H_y^2 + H_z^2}$$

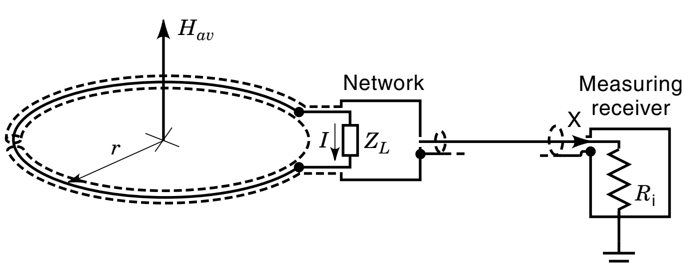

Figure 5. Magnetic field strength measuring loop. The network may consist of a passive or active circuit.

Isotropic performance is however only a reality in broadband magnetic field sensors, where each component is detected with a square-law detector and combined subsequently. For the measurement and detection of radio signals isotropic antennas are not available. Hybrids may be used for limited fre-

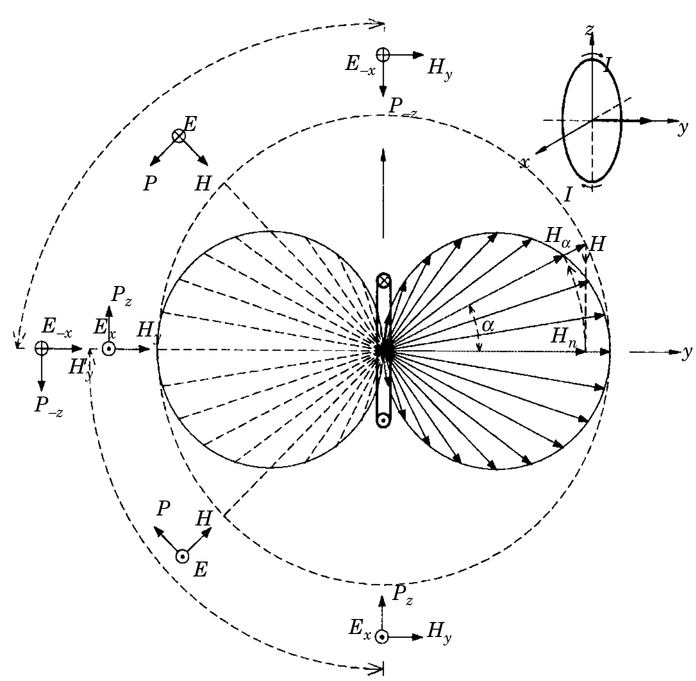

Figure 6. Cross section of a loop antenna sensitivity pattern. The arrow length H_α shows the indicated field strength at an angle α which is a fraction of the original field strength H, with $H_\alpha = H \cos \alpha$.

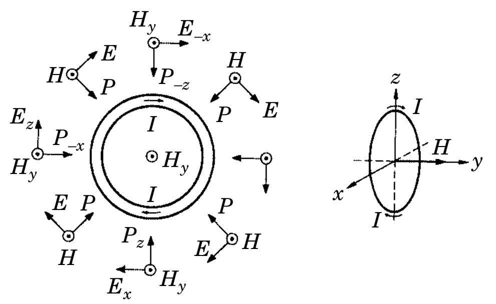

Figure 7. Direction of the field vectors (H, E, and P) under far-field conditions.

quency ranges to achieve an omnidirectional azimuthal (not isotropic) pickup.

Antenna-Factor Definition. The output voltage V of a loop antenna is proportional to the average magnetic field strength H perpendicular to the loop area. If the antenna output is connected to a measuring receiver or a spectrum analyzer, the set consisting of antenna and receiver forms a selective magnetometer.

The proportionality constant is the antenna factor K_H for the average magnetic field strength H:

$$K_H = \frac{H}{V} \quad \text{in} \quad \frac{\text{A}}{\text{m}}\frac{1}{\text{V}} = \frac{1}{\Omega\text{m}} \tag{1a}$$

For the average magnetic flux density B the corresponding proportionality constant is

$$K_B = \frac{B}{V} = \frac{\mu_0 H}{V} = \mu_0 K_H \quad \text{in} \quad \frac{\text{Vs}}{\text{Am}}\frac{\text{A}}{\text{m}}\frac{1}{\text{V}} = \frac{\text{Vs}}{\text{m}^2}\frac{1}{\text{V}} = \frac{\text{T}}{\text{V}} \tag{1b}$$

In the far field, where electric field and magnetic fields are related via the free-space wave impedance Z_0, the loop antenna can be used to determine the electric field strength E. For this case the proportionality constant is:

$$K_E = \frac{E}{V} = \frac{Z_0 H}{V} = Z_0 K_H \quad \text{in} \quad \frac{\text{V}}{\text{A}}\frac{\text{A}}{\text{m}}\frac{1}{\text{V}} = \frac{1}{\text{m}} \tag{1c}$$

In the area of radio wave propagation and radio disturbance measurement, quantities are expressed in logarithmic units. Therefore, the proportionality constants are converted into logarithmic values too:

$$k_H = 20\log(K_H) \quad \text{in} \quad \text{dB}\left(\frac{1}{\Omega\text{m}}\right) \tag{2a}$$

$$k_B = 20\log(K_B) \quad \text{in} \quad \text{dB}\left(\frac{\text{T}}{\text{V}}\right) \tag{2b}$$

$$k_E = 20\log(K_E) \quad \text{in} \quad \text{dB}\left(\frac{1}{\text{m}}\right) \tag{2c}$$

By using logarithmic antenna factors, a field-strength level $20\log(H)$ is obtained in dB(μA/m) from the measured output voltage level $20\log(V)$ in dB(μV) by applying the equation: $20\log(H) = 20\log(V) + k_H$. The final section of this article describes a method to calibrate the antenna factors of circular loop antennas.

Concepts of Magnetic Field-Strength Meters. The loop antenna of a magnetic field-strength meter may be mounted on the measuring receiver or used as a separate unit, connected to the measuring receiver with a coaxial cable. CISPR 16-1, the basic standard for emission measurement instrumentation to commercial (i.e., nonmilitary) standards, requires a loop antenna in the frequency range of 9 kHz to 30 MHz which is completely enclosed by a square having sides 0.6 m in length. For protection against stray pick-up of electric fields, loop antennas employ a coaxial shielding structure. For optimum performance, the shielding structure may be arranged symmetrically in two half-circles around a circular loop with a slit between the two halves in order to avoid electric contact between the two shields.

For narrowband magnetic field measurements of radio disturbance, measuring receivers employ standardized bandwidths and weighting detectors in order to produce standardized measurement results for all types of perturbations including impulsive signals. For comparison with the emission limit, usually the quasi-peak (QP) detector is to be used.

To understand the function of a weighting curve in measuring receivers, the following interpretation is given. The test receiver has certain elements that determine a weighting curve (e.g. for the QP detector): the measurement bandwidth, the charge and discharge times of the detector circuit, and the time constant of the meter. When measured with a QP detector, for the frequency range given in Fig. 8, an impulsive signal with a constant impulse strength and a pulse repetition frequency of 100 Hz will cause a meter indication 10 dB above that of the indication when the pulse repetition frequency is 10 Hz. Or, to produce the same indication on the meter as a signal with 100-Hz repetition frequency, the level of the 10-Hz impulsive signal will have to be increased by an amount of 10 dB.

Earlier manually operated field-strength meters achieved high sensitivity by operating the loop at resonance (14). The sensitivity was raised by the amount of the Q-factor of the resonating circuit. One of the latest models which was used up to the 1980s, reached a sensitivity of -60 dB(μA/m) with a measurement bandwidth of 200 Hz in the frequency range 100 kHz to 30 MHz (15).

For automated field-strength measurement systems, tuning of the loop circuit could no longer be afforded. A broad-

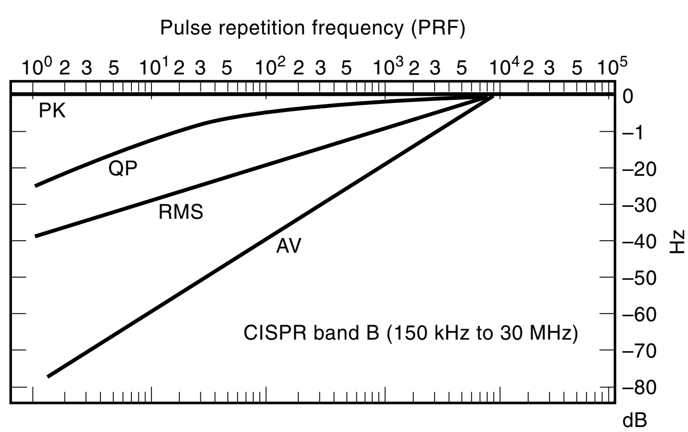

Figure 8. Detector response of a test receiver for impulsive interference as specified in Ref. 1.

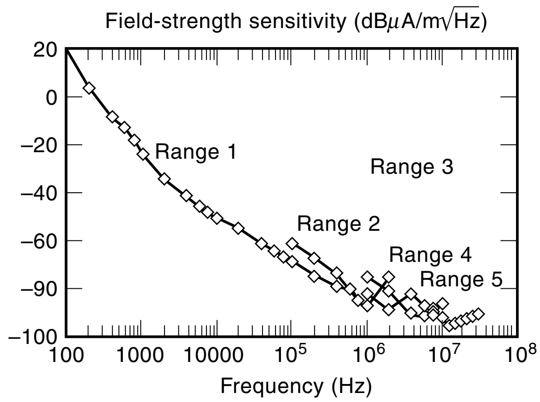

Figure 9. Sensitivity per hertz bandwidth of the active loop (16).

band active loop employs an output voltage proportional to the short-circuited loop current thus achieving a flat response of the antenna factor versus frequency (16).

A flat response of the system is also achieved using a current probe which measures the short-circuit current in the large-loop antenna system (LAS) described by Bergervoet and van Veen (9). It is essentially a magnetic-field-induced current measurement (see subsequent explanations). The highest sensitivity described in the literature for a wideband system was achieved with a specially designed active loop. With additional frequency-dependant switching of elements (17) sensitivity is even better than that of manually operated field-strength meters with tuning of the loop circuit. Figure 9 shows the amplitude density of the minimum detectable magnetic field strength H_{Neq} in dB(μA/m$\sqrt{\text{Hz}}$) equivalent to the internal electronic noise of the system consisting of antenna and measuring receiver.

MAGNETIC-FIELD-STRENGTH MEASUREMENT METHODS

Measurement of Magnetic Fields With Regard to Human Exposure to High em Fields

Usually, to measure magnetic fields with regard to human exposure to high fields, magnetic field-strength meters are using broadband detectors and apply an isotropic response. Modern concepts of low-frequency electric and magnetic field strength meters apply fast Fourier transform (FFT) for proper weighting of the total field with regard to frequency-dependent limits (18,19).

Use of Loop Antennas for Radio Wave Field-Strength Measurements Up to 30 MHz

ITU-R Recommendation PI.845-1 Annex 1 gives guidance to accurate measurement of radio wave field strengths. Rod antennas are the preferred receiving antennas since they provide omnidirectional azimuthal pickup. The positioning of vertical rod antennas is however important, since the result is very sensitive to field distortions by obstacles and sensitive to the effects of ground conductivity. It is a well-known fact that measurements with loop antennas are less sensitive to these effects and their calibration is not affected by ground conductivity apart from the fact that the polarization may deviate from horizontal if ground conductivity is poor. Therefore, many organizations use vertical monopoles for signal measurements but standardize results by means of calibration data involving comparisons for selected signals indicated by field-strength meters incorporating loop-receiving antennas. Accuracy requirements are given in Ref. 20, general information on equipment and methods of radio monitoring are given in Ref. 21.

Solutions to Problems With Ambients in Commercial EMI Standards. CISPR Class B radiated emission limits in the frequency range 9 kHz to 30 MHz have been at 34 dB(μV/m) at a distance of 30 m from the EUT for a long time. Moreover, the test setup with EUT and vertical loop antenna required turning of both EUT and loop antenna in order to find the maximum emission. On most of the open area test sites the ambient noise level makes compliance testing almost impossible. This is due to the fact that ambient noise itself is near or above the emission limit. Two different approaches were proposed as a solution to that problem:

(1) To reduce the measurement distance from 30 m to 10 m or even 3 m. A German group proposed frequency-dependent conversion factors, justified by calculations and an extensive amount of measurements. The conversion factors are given in Fig. 10. In Fig. 10 the slopes between 1.8 MHz and 16 MHz show the transition region from near field, where H is inversely proportional with r^3 or $r^{2.6}$, to far field, where H is inversely proportional with r.

(2) To reduce the measurement distance to zero. A Dutch group proposed the large-loop antenna system mentioned previously (9). With this method the EUT is placed in the center of a loop antenna system, which consists of three mutually perpendicular large loop antennas (Fig. 11). The magnetic field emitted by the EUT induces currents in the large loop antennas. Since there are three orthogonal loops, there is no need to rotate either the EUT or the loop antenna system. The current induced in each loop is measured by means of a current probe, which is connected to a CISPR measuring re-

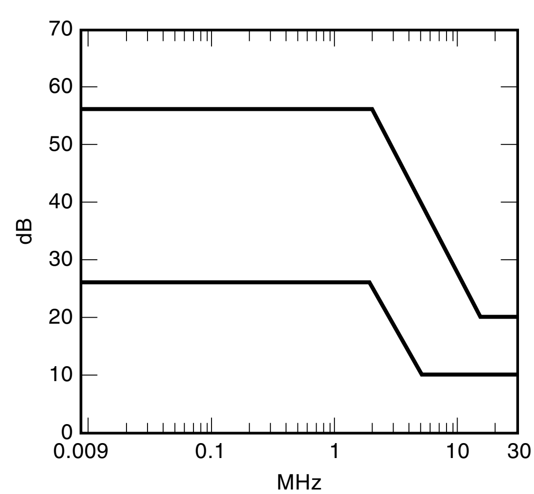

Figure 10. Conversion factors ΔH for the limit of the magnetic field strength from 30-m measurement distance to 10-m and 3-m measurement distances above a conducting ground plane according to Ref. 26. The upper curve is for 30 to 3 m, the lower curve is for 30 to 10 m distances.

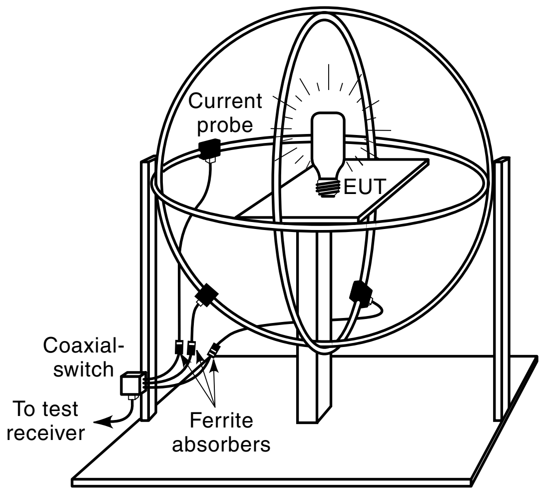

Figure 11. Simplified drawing of a large loop antenna system with position of the EUT.

ceiver. Since the current is measured, emission limits are given in dB(μA) instead of dB(μA/m). Each loop antenna is constructed of a coaxial cable which contains two slits, positioned symmetrically with respect to the position of the current probe. Each slit is loaded by resistors in order to achieve a frequency response flat to within ±2 dB in the frequency range from 9 kHz to 30 MHz (9,10). In order to verify and validate the function of each large loop, a specially designed folded dipole has been developed (9,10). It produces both a magnetic dipole moment m_H and an electric dipole moment m_E, when a signal is connected to the folded dipole. The folded dipole serves to test the large loop antenna for its sensitivity in 8 positions.

Problems in the Near Field to Far Field Transition Zone. Problems with magnetic field strength measurements in the transition region between near field and far field are discussed in detail in Ref. 22. When a small magnetic dipole is located in the free space, the electromagnetic field in a point $P(r, \theta, \varphi)$ is described by the following three relations (see Fig. 12):

$$H_r = \frac{jk}{2\pi}\frac{m_H\cos\theta}{r^2}\left(1+\frac{1}{jkr}\right)e^{-jkr} \tag{3a}$$

$$H_\theta = \frac{-k^2}{4\pi}\frac{m_H\sin\theta}{r}\left(1+\frac{1}{jkr}-\frac{1}{(kr)^2}\right)e^{-jkr} \tag{3b}$$

$$E_\varphi = \frac{Z_0k^2}{4\pi}\frac{m_H\sin\theta}{r}\left(1+\frac{1}{jkr}\right)e^{-jkr} \tag{3c}$$

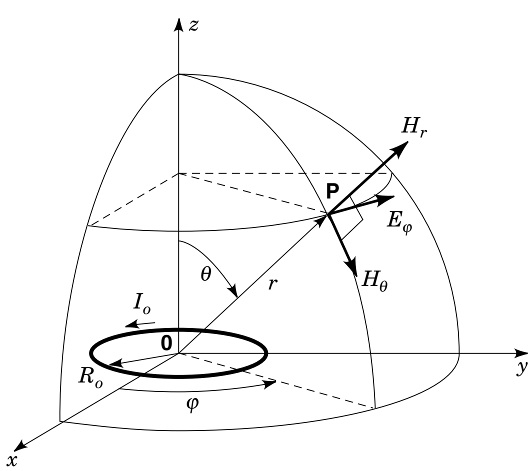

Figure 12. Field components H_r, H_θ, and E_φ in **P** at a distance $r$from the center of the magnetic dipole in the xy-plane.

where $k = 2\pi/\lambda$, and $m_H = \pi R_0^2 I_0$ is the magnetic dipole moment, a vector perpendicular to the plane of the dipole. Equations (3a–3c) completely describe the electromagnetic field of the magnetic dipole.

Two situations are further discussed: (1) the near field, where r is much smaller than λ but larger than the maximum dimension of the source (i.e. $kr \ll 1$), and (2) the far field, where r is much larger than λ and much larger than the maximum dimension of the source (i.e. $kr \gg 1$).

For the near field case, where $kr \ll 1$ and using $e^{-jkr} = \cos(kr) - j\sin(kr)$, Eqs. (3a–3c) are simplified to

$$H_r = \frac{2m_H\cos\theta}{4\pi r^3} \tag{4a}$$

$$H_\theta = \frac{m_H\sin\theta}{4\pi r^3} \tag{4b}$$

$$E_\varphi = \frac{kZ_0m_H\sin\theta}{4\pi r^2} \tag{4c}$$

From Eqs. (4a–4c) we can see that H_r and H_θ are inversely proportional to r^3, whereas E_φ is inversely proportional to r^2.

For the far-field case where $kr \gg 1$, Eqs. (3a–3c) are reduced to

$$H_r = \frac{jkm_H\cos\theta}{2\pi r^2}e^{-jkr} \Rightarrow 0 \tag{5a}$$

$$H_\theta = \frac{-k^2m_H\sin\theta}{4\pi r}e^{-jkr} \tag{5b}$$

$$E_\varphi = \frac{k^2Z_0m_H\sin\theta}{4\pi r}e^{-ikr} \tag{5c}$$

From Eqs. (5a–5c) one can see that in the far field H_r vanishes in comparison to H_θ and that H_θ and E_φ are inversely proportional to r.

In the frequency range of 9 kHz to 30 MHz, where emission limits have been set, the corresponding wavelength is 33 km to 10 m. Since for compliance testing, ambient emissions on an open area test site require a reduction of the measurement distance to 10 m or even 3m, measurements are carried out in the near field zone over a wide frequency range. At the higher frequency range the transition zone and the beginning far field zone are reached. Goedbloed (22) investigated the transition zone and identified the critical condition where H_r and H_θ are equal in magnitude. It occurs where

$$\frac{2m_H}{4\pi r^3}\sqrt{1+k^2r^2} = \frac{m_H}{4\pi r^3}\sqrt{1-k^2r^2+k^4r^4} \tag{6}$$

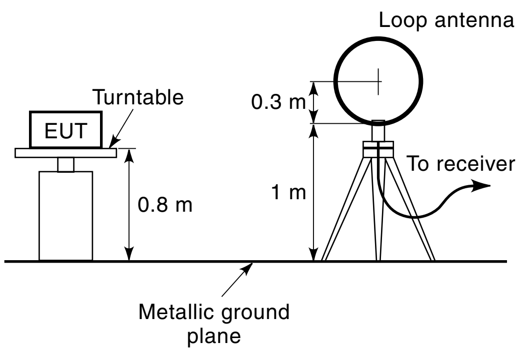

Figure 13. Basic CISPR setup for magnetic field measurements. Both EUT and loop antennas have to be turned round until the maximum indication on the receiver has been found.

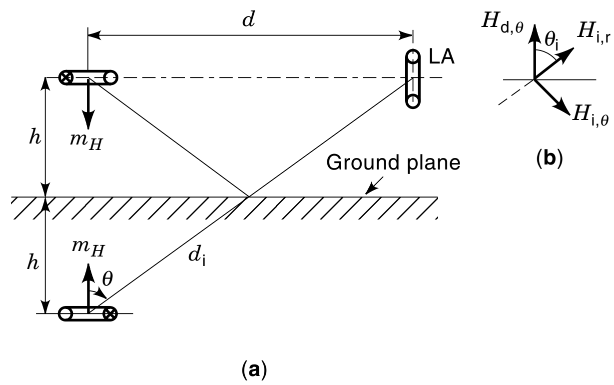

Figure 15. (a) Receiving conditions for a magnetic dipole with a vertical dipole moment, and the receiving loop-antenna in the vertical position as specified by the standard; (b) Vectors of the indirect radiated H-field components (no reception of direct radiation).

or where

$$fr = 112.3 \quad \text{in} \quad \text{MHz} \cdot \text{m} \tag{7}$$

For $r = 10$ m, $H_{\theta\max} > H_{r\max}$ at frequencies greater than 11 MHz.

The CISPR magnetic field measurement method is illustrated by Fig. 13, with the test setup on a metallic ground plane and the receiving antenna in the vertical plane. In Figs. 14 and 15, two different cases of radiating electrically small magnetic dipoles are illustrated: the first one with the dipole moment parallel to the ground plane and the second one with the dipole moment perpendicular to the ground plane. Because of the reflecting ground plane two sources are responsible for the field at the location of the receiving antenna: the original source and the mirror source. The points and crosses drawn in both sources show the direction of the current. In Fig. 14, the currents are equally oriented. In this case the loop antenna detects the radial component $H_{\mathrm{d,r}}$ and the direct tangential component $H_{\mathrm{d},\theta} = 0$ since $\theta_{\mathrm{d}} = 0$. Therefore, direct radiation will only contribute if $fd \ll 112$ MHz · m, see Eq. (7). In the case of $fd \gg 112$ MHz · m, the loop antenna will receive direct radiation if it is rotated by 90°. This may be observed frequently in practical measurements: at low frequencies the maximum radiation is found with the loop antenna in parallel to the EUT and at high frequencies with the loop antenna oriented perpendicular to the EUT. In addition to these direct components, the indirect radial and tangential components $H_{\mathrm{i,r}}$ and $H_{\mathrm{i},\theta}$ are superpositioned in the loop antenna. Assuming near-field conditions it follows from Eqs. (4), that the magnitude of the magnetic field H_{m} is given by

$$\begin{aligned} H_m &= H_{d,r} + H_{i,r}\cos\theta_i - H_{i,\theta}\sin\theta_i \\ &= \frac{m_H}{4\pi d^3}\left(2 + \frac{d^3}{d_i^3}(2\cos^2\theta_i - \sin^2\theta_i)\right) \end{aligned} \tag{8}$$

where $d_i = \sqrt{(2h)^2 + d^2}$ is the distance between the mirror dipole and the loop antenna.

Goedbloed gives a numerical example with $m_{\mathrm{H}} = 4\pi 10^3$ μAm^2 (e.g. 100 mA through a circular loop with a diameter of 0.40 m). Using Eq. (8) with $d = 3$ m and $h = 1.3$ m will give $H_{\mathrm{m}} = 38.6$ dB(μA/m) with the mirror source and 37.4 dB(μA/m) without the mirror source, which shows that in this case the reflecting ground plane has little influence. The influence of the ground plane is quite different in the case of a vertical dipole moment, i.e. a dipole moment perpendicular to the ground plane as illustrated in Fig. 15. In the case of Fig. 15 the loop antenna does not receive direct radiation at all, as $H_{\mathrm{d,r}}$ ($\theta_{\mathrm{d}} = \pi/2$) = 0 and $H_{\mathrm{d},\theta}$ is parallel to the loop antenna. Hence, the received signal is completely determined by the radiation coming from the mirror source, which also means that the result is determined by the quality of the reflecting ground plane. With the reflecting ground plane $H_m = H_{i,r}$ sin θ_i + $H_{i,\theta}$ cos θ_i = 27.2 dB(μA/m), whereas without the reflecting ground plane no field strength will be measured. If the loop antenna were positioned horizontally above the ground plane at $h = 1.3$ m, $H_m = H_{d,\theta} + H_{i,r}$ cos θ_i − $H_{i,\theta}$ sin θ_i = 32.4 dB(μA/m) and $H_{\mathrm{m}} = 31.4$ dB(μA/m) without the reflecting ground plane. Measurements in a shielded room would even be less predictable, since the result would be determined by mirror sources on each side including the ceiling of the shielded room. Absorbers are not very helpful in the low frequency ranges. From these results, Goedbloed concludes that in order to judge the interference capability of an EUT, the method proposed by Bergervoet and Van Veen (9), is an efficient method of magnetic field measurements.

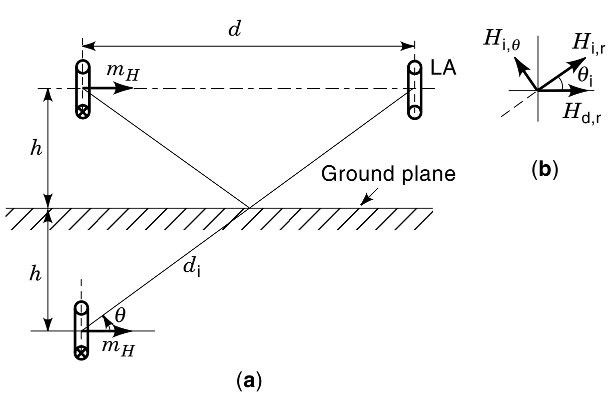

Figure 14. (a) Receiving conditions for a magnetic dipole with a horizontal dipole moment; (b) Vectors of the direct and indirect radiated H-field components.

CALIBRATION OF A CIRCULAR LOOP ANTENNA

A time-varying magnetic field at a defined area S can be determined with a calibrated circular loop. For narrow-band magnetic field measurements, a measuring loop consists of an output interface (point **X** on Fig. 5), which links the induced current to a measuring receiver. It may have a passive or an active network between loop terminals and output. The measuring loop can also include a shielding over the loop circumference against any perturbation of strong and unwanted electric fields. The shielding should be interrupted at a point on the loop circumference.

Generally in the far-field the streamlines of magnetic flux are uniform, but in the near-field, i.e. in the vicinity of the generator of a magnetic field, they depend on the source and its periphery. Figure 19 shows the streamlines of the electromagnetic vectors generated by the transmitting loop **L1**. In the near-field, the spatial distribution of the magnetic flux, $B = \mu_0 H$, over the measuring loop area is not known. Only the normal components of the magnetic flux, averaged over the closed-loop area, can induce a current through the loop conductor.

The measuring loop must have a calibration (conversion) factor or set of factors, that, at each frequency, expresses the relationship between the field strength impinging on the loop and the indication of the measuring receiver. The calibration of a measuring loop requires the generation of a well-defined standard magnetic field on its effective receiving surface. Such a magnetic field is generated by a circular transmitting loop when a defined root mean square (rms) current is passed through its conductor. The unit of the generated or measured magnetic field H_{av} is A/m and therefore is also an rms value. The subscript, av, strictly indicates the average value of the spatial distribution, not the average over a period of T of a periodic function. This statement is important for near-field calibration and measuring purposes. For far-field measurements the result indicates the rms value of the magnitude of the uniform field. In the following we discuss the requirements for the near-zone calibration of a measuring loop.

CALCULATION OF STANDARD NEAR-ZONE MAGNETIC FIELDS

To generate a standard magnetic field, a transmitting loop **L1** is positioned coaxial and plane-parallel at a separation distance d from the loop **L2**, like in Fig. 16. The analytical formula for the calculation of the average magnetic field strength H_{av} in A/m generated by a circular filamentary loop at an axial distance d including the retardation due to the finite propagation time was obtained earlier by Greene (23). The average value of field strength H_{av} was derived from the retarded vector potential A_φ as tangential component on the point P of the periphery of loop **L2**:

$$H_{\text{av}} = \frac{Ir_1}{\pi r_2} \int_0^{\pi} \frac{e^{-j\beta R(\varphi)}}{R(\varphi)} \cos(\varphi) d\varphi \tag{9a}$$

$$R(\varphi) = \sqrt{d^2 + r_1^2 + r_2^2 - 2r_1 r_2 \cos(\varphi)} \tag{9b}$$

In these equations for the thin circular loop, I is transmitting loop rms current in A, d is distance between the planes

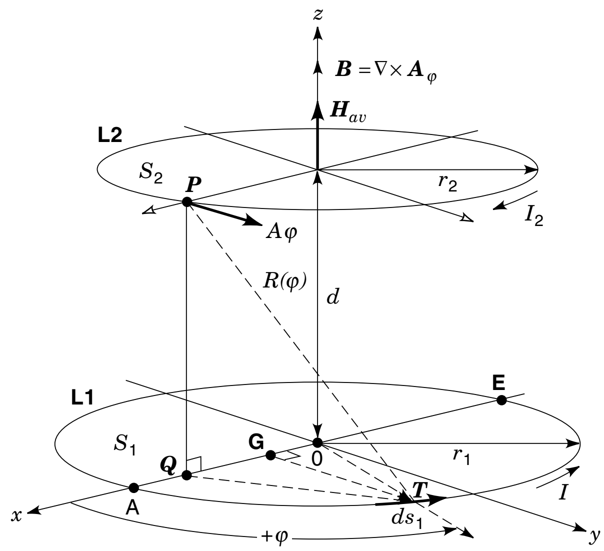

Figure 16. Configuration of two circular loops.

of the two coaxial loop antennas in m, r_1 and r_2 are filamentary loop radii of transmitting and receiving loops in m, respectively, β is wavelength constant, $\beta = 2\pi/\lambda$, and λ is wavelength in m.

Equations (9a) and (9b) can be determined by numerical integration. To this end we separate the real and imaginary parts of the integrand using Euler's formula $e^{-j\varphi} = \cos(\varphi) - j \sin(\varphi)$ and rewrite Eq. (9a) as

$$H_{av} = \frac{Ir_1}{\pi r_2}(F - jG) \tag{10a}$$

where

$$F = \int_0^{\pi} \frac{\cos[\beta R(\varphi)]}{R(\varphi)} \cos(\varphi) d\varphi \tag{10b}$$

$$G = \int_0^{\pi} \frac{\sin[\beta R(\varphi)]}{R(\varphi)} \cos(\varphi) d\varphi \tag{10c}$$

and the magnitude of H_{av} is then obtained as

$$|H_{\text{av}}| = \frac{Ir_1}{\pi r_2}\sqrt{F^2 + G^2} \tag{10d}$$

It is possible to evaluate the integrals in Eqs. (10) by numerical integration with an appropriate mathematics software on a personal computer. Some mathematics software can directly calculate the complex integral of Eqs. (9).

ELECTRICAL PROPERTIES OF CIRCULAR LOOPS

Current Distribution Around a Loop

The current distribution around the transmitting loop is not constant in amplitude and in phase. A standing wave of current exists on the circumference of the loop. This current distribution along the loop circumference is discussed by Greene on pp. 323–324 (23). He has assumed the loop circumference $2\pi r_1$ being electrically smaller than the wave length λ and the

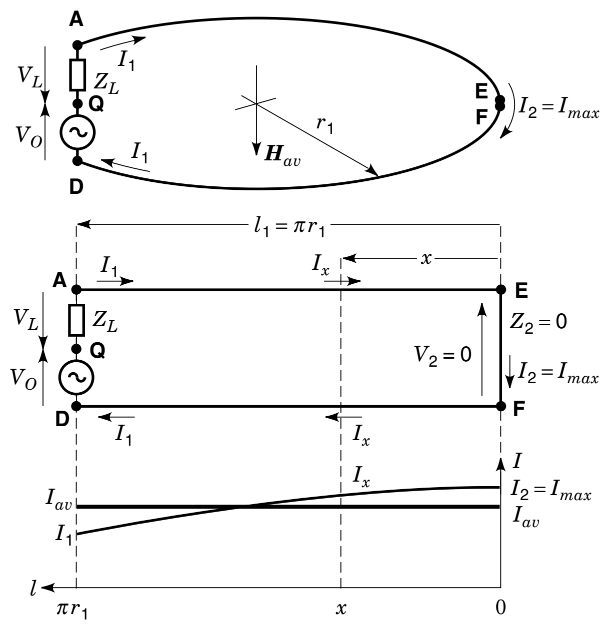

Figure 17. Current distribution on a circular loop.

loop current being constant in phase around the loop and the loop being sufficiently loss-free. The single-turn thin loop was considered as a circular balanced transmission line fed at points **A** and **D** and short-circuited at the points **E** and **F** (Fig. 17).

In an actual calibration setup the loop current I_1 is specified at the terminals **A** and **D**. The average current was given as a function of input current I_1 of the loop (24):

$$I_{\mathrm{av}} = I_1 \frac{\tan(\beta\pi r_1)}{\beta\pi r_1} \tag{11}$$

The fraction of I_{av}/I_1 from Eq. (11) expressed in dB gives the conditions for determining of the highest frequency f and the radius of the loop r_1. The deviation of this fraction is plotted in Fig. 18.

The current I in Eqs. (9) must be substituted with I_{av} from Eq. (11). Since Eq. (11) is an approximate expression, it is recommended to keep the radius of the transmitting loop small enough for the highest frequency of calibration to minimize the errors. For the dimensioning of the radius of the receiving loop these conditions are not very important, until

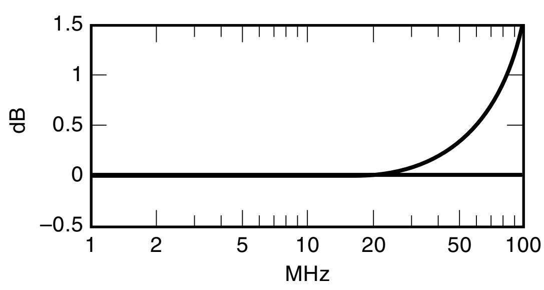

Figure 18. Deviation of I_{av}/I_1 for a loop radius, 0.1 m as 20 $\log(I_{av}/I_1)$ in dB versus frequency.

the receiving loop is calibrated with an accurately defined standard magnetic field, but the resonance of the loop at higher frequencies must be taken into account.

Circular Loops With Finite Conductor Radii

A measuring loop can be constructed with one or more winding. The form of the loop is chosen as a circle, because of the simplicity of the theoretical calculation and calibration. The loop conductor has a finite radius. At high frequencies the loop current flows on the conductor surface and it shows the same proximity effect as two parallel, infinitely long cylindrical conductors. Figure 19 shows the cross-section of two loops intentionally in exaggerated dimensions. The streamlines of the electric field are orthogonal to the conductor surface of the transmitting loop **L1** and they intersect at points **A** and **A′**. The total conductor current is assumed to flow through an equivalent thin filamentary loop with the radius $a_1 = \sqrt{r_1^2 - c_1^2}$, where $a_1 = \overline{\mathbf{OA}} = \overline{\mathbf{OP}} = \sqrt{\overline{\mathbf{OQ}}^2 - \overline{\mathbf{QP}}^2}$. The streamlines of the magnetic field are orthogonal to the streamlines of electric field. The receiving loop **L2** with the finite conductor radius c_2 can encircle a part of magnetic field with its effective circular radius $b_2 = r_2 - c_2$.

The sum of the normal component of vectors H acting on the effective receiving area $S_2 = \pi b_2^2$ induces a current in the conductor of the receiving loop **L2**. This current flows through the filamentary loop with the radius a_2. The average magnetic field vector H_{av} is defined as the integral of vectors H_n over effective receiving area S_2, divided by S_2. The magnetic streamlines, which flow through the conductor and outside of loop **L2**, cannot induce a current through the conductor along the filamentary loop **Ar**, **Ar′**, of **L2**. The equivalent filamentary loop radii a_1, a_2 and effective circular surface radii b_1, b_2 can directly be seen from Fig. 19.

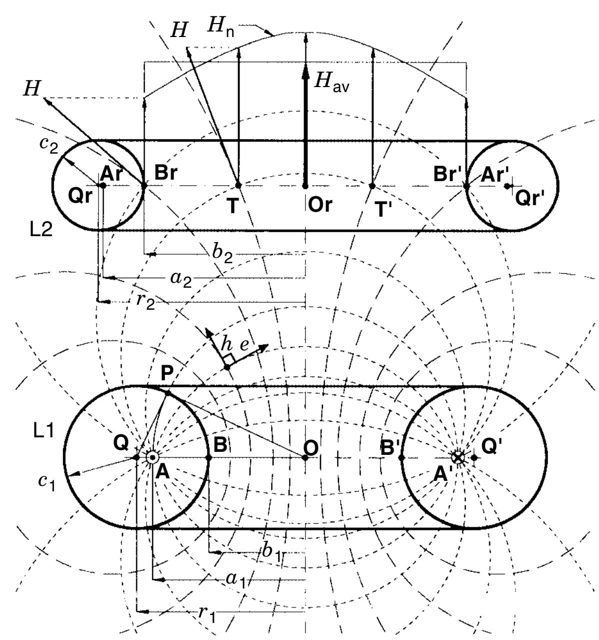

Figure 19. Filamentary loops of two loops with finite conductor radii and orthogonal streamlines of the electromagnetic vectors, produced from transmitting loop **L1**.

The equivalent thin current filament radius a_1 of the transmitting loop **L1**:

$$a_1 = \sqrt{r_1^2 - c_1^2} \tag{12a}$$

The equivalent thin current filament radius a_2 of the receiving loop **L2**:

$$a_2 = \sqrt{r_2^2 - c_2^2} \tag{12b}$$

The radius b_1 of the effective receiving circular area of the loop transmitting **L1**:

$$b_1 = r_1 - c_1 \tag{12c}$$

The radius b_2 of the effective receiving circular area of the receiving loop **L2**:

$$b_2 = r_2 - c_2 \tag{12d}$$

Impedance of a Circular Loop

The impedance of a loop can be defined at chosen terminals **Q**, **D**, as $Z = V/I_1$ (Fig. 17). Using Maxwell's equation with the Faraday's law curl$\boldsymbol{E} = -j\omega\Phi_m$ we can write the line integrals of the electric intensity E along the loop conductor through its cross section, along the path joining points **D**, **Q**, and the load impedance Z_L between the terminals **Q**, **A**:

$$\int_{(AEFD)} E_s ds + \int_{(DQ)} E_s ds + \int_{(QA)} E_s ds = -j\omega\Phi_m \tag{13a}$$

Here, Φ_m is the magnetic flux. The impressed emf V acting along the path joining points **D** and **Q** is equal and opposite to the second term of Eq. (13a):

$$V = -\int_{(DQ)} E_s ds \tag{13b}$$

The impedance of the loop at the terminals **D**, **Q** can be written from Eqs. (13) dividing with I_1 as

$$Z = \frac{V}{I_1} = \frac{\int_{(AEFD)} E_s ds}{I_1} + \frac{\int_{(QA)} E_s ds}{I_1} + \frac{j\omega\Phi_m}{I_1} = Z_i + Z_L + Z_e \tag{14}$$

Z_i indicates the internal impedance of the loop conductor. Because of the skin effect, the internal impedance at high frequencies is not resistive. For the calculation of the Z_i we refer to Schelkunoff, p. 262 (25). Z_L is a known load or a source impedance on Fig. 17. Z_e is the external impedance of the loop:

$$Z_e = j\omega\frac{\Phi_m}{I_1} = j\omega\frac{\mu_0 H_{av} S}{I_1} \tag{15a}$$

We can consider that the loop consists of two coaxial and coplanar filamentary loops (i.e. separation distance $d = 0$). The radii a_1 and b_1 are defined in Eqs. (12). The average current I_{av} flows through the filamentary loop with the radius a_1 and generates an average magnetic field strength H_{av} on the effective circular surface $S_1 = \pi b_1^2$ of the filamentary loop with the radius b_1. From the Eqs. (9) and (11) we can rewrite Eq. (15a), for the loop **L1**:

$$Z_e = j\frac{\tan(\beta\pi a_1)}{\beta\pi a_1}\mu_0\omega a_1 b_1 \int_0^\pi \frac{e^{-j\beta R_0(\varphi)}}{R_0(\varphi)}\cos(\varphi)d\varphi \tag{15b}$$

$$R_0(\varphi) = \sqrt{a_1^2 + b_1^2 - 2a_1 b_1 \cos(\varphi)} \tag{15c}$$

The real and imaginary parts of Z_e are the radiation resistance and the external inductance of loops, respectively:

$$\mathrm{Re}(Z_e) = \frac{\tan(\beta\pi a_1)}{\beta\pi a_1}\mu_0\omega a_1 b_1 \int_0^\pi \frac{\sin(\beta R_0(\varphi))}{R_0(\varphi)}\cos(\varphi)d\varphi \tag{15d}$$

$$\mathrm{Im}(Z_e) = \frac{\tan(\beta\pi a_1)}{\beta\pi a_1}\mu_0\omega a_1 b_1 \int_0^\pi \frac{\cos(\beta R_0(\varphi))}{R_0(\varphi)}\cos(\varphi)d\varphi \tag{15e}$$

From Eq. (15e) we obtain the external self inductance:

$$L_e = \frac{\tan(\beta\pi a_1)}{\beta\pi a_1}\mu_0 a_1 b_1 \int_0^\pi \frac{\cos(\beta R_0(\varphi))}{R_0(\varphi)}\cos(\varphi)d\varphi \tag{15f}$$

Equations 15 include the effect of current distribution on the loop with finite conductor radii.

Mutual Impedance Between Two Circular Loops

The mutual impedance Z_{12} between two loops is defined as

$$Z_{12} = \frac{V_2}{I_1} = \frac{Z_2 I_2}{I_1} \tag{16}$$

The impedance of Z_2 in Eq. (16) can be defined like Eq. (14):

$$Z_2 = \frac{V_2}{I_2} = Z_{2i} + Z_L + Z_{2e} \tag{17}$$

here Z_{2i} is the internal impedance, Z_L is the load impedance, and Z_{2e} is the external impedance of the second loop **L2**.

The current ratio I_2 to I_1 in Eq. (16) can be calculated from Eqs. (9), (11), and (12). The current I_1 of the transmit loop with separation distance d:

$$I_1 = \frac{H_{av}\pi b_2}{\frac{\tan(\beta\pi r a_1)}{\beta\pi a_1} a_1 \int_0^\pi \frac{e^{-j\beta R_d(\varphi)}}{R_d(\varphi)}\cos(\varphi)d\varphi} \tag{18a}$$

$$R_d(\varphi) = \sqrt{d^2 + a_1^2 + b_2^2 - 2a_1 b_2 \cos(\varphi)} \tag{18b}$$

and the current I_2 of the receive loop for the same H_{av} (here $d = 0$) is

$$I_2 = \frac{H_{av}\pi b_2}{\frac{\tan(\beta\pi a_2)}{\beta\pi a_2} a_2 \int_0^\pi \frac{e^{-j\beta R_0(\varphi)}}{R_0(\varphi)}\cos(\varphi)d\varphi} \tag{18c}$$

$$R_0(\varphi) = \sqrt{a_2^2 + b_2^2 - 2a_2 b_2 \cos(\varphi)} \tag{18d}$$

The general mutual impedance between two loops from Eqs. (16) and (17) is

$$Z_{12} = (Z_{2i} + Z_L + Z_{2e})\frac{I_2}{I_1} = Z_{12i} + Z_{12L} + Z_{12e} \quad (19a)$$

here Z_{12i} is the mutual internal impedance, Z_{12L} denotes the mutual load impedance, and Z_{12e} is the external mutual impedance.

Arranging Eq. (15b) for Z_{2e} and the current ratio I_2/I_1 from Eqs. (18) external mutual impedance yield

$$Z_{12e} = j\frac{\tan(\beta\pi a_1)}{\beta\pi a_1}\mu_0\omega a_1 b_2 \int_0^{\pi} \frac{e^{-j\beta R_d(\varphi)}}{R_d(\varphi)}\cos(\varphi)d\varphi \quad (19b)$$

The real part of Z_{12e} may be described as mutual radiation resistance between two loops.

The imaginary part of Z_{12e} divided by ω gives the mutual inductance

$$M_{12e} = \frac{\tan(\beta\pi a_1)}{\beta\pi a_1}\mu_0 a_1 b_2 \int_0^{\pi} \frac{\cos(\beta R_d(\varphi))}{R_d(\varphi)}\cos(\varphi)d\varphi \quad (19c)$$

Equations (19b) and (19c) include the effect of current distribution on the loop with finite conductor radii.

DETERMINATION OF THE ANTENNA FACTOR

The antenna factor K is defined as a proportionality constant with necessary conversion of units. K is the ratio of the average magnetic field strength bounded by the loop to the measured output voltage V_L on the input impedance R_L of the measuring receiver. For the evaluation of the antenna factor there are two methods. The first is by calculation of the loop impedances, and the second is with the well-defined standard magnetic field calibration, which will also be needed for the verification of calculated antenna factors (24).

Determination of the Antenna Factor by Computing from the Loop Impedances

If a measurement loop (e.g. **L2**) has a simple geometric shape and a simple connection to a voltage measuring device with a known load R_L, we can determine the antenna factor by calculation. In the case of unloaded loop from Fig. 17 the open circuit voltage is

$$V_0 = j\omega\mu_0 H_{\mathrm{av}} S_2 \quad (20a)$$

For the case of loaded loop the current is

$$I = \frac{V_0}{Z} = \frac{V_0}{R_L + Z_i + Z_e} \quad (20b)$$

The antenna factor from Eq. (9a) can be written with $V_L = Z_L I$ and Eqs. (20) as

$$K_H = \left|\frac{1}{j\omega\mu_0 S_2}\left(1 + \frac{Z_e}{R_L} + \frac{Z_i}{R_L}\right)\right| \quad \text{in} \quad \frac{\mathrm{A}}{\mathrm{m}}\frac{1}{\mathrm{V}} \quad (21)$$

The effective loop area is $S_2 = \pi b_2^2$. The external loop impedance Z_e can be calculated with Eqs. (15). The internal impedance Z_i can be evaluated from Ref. 25.

Standard Magnetic Field Method

In the calibration setup in Fig. 20 we measure the voltages with standard laboratory measuring instrumentation with the 50 Ω impedance. The device to be calibrated consists at least of a loop and a cable with an output connector. Such a measuring loop can also include a passive or active network between the terminals **C**, **D**, and a coaxial shield on the circular loop conductor against unwanted electric fields, depending on its development and construction. The impedance Z_L at the terminals **C**, **D** is not accurately measurable. Such a complex loop must be calibrated with the standard magnetic field method. The antenna factor in Eqs. (1) can be defined through measuring of the voltage V_L and the uncertainties between loop terminals **C**, **D** and measuring receiver are fully calibrated. The attenuation ratio α of the voltages V_2 and V_L can be measured for each frequency:

$$\alpha = \frac{V_2}{V_L} \quad (22)$$

By using the Eqs. (22), (1), (11), and (12), with $V_2 = -I_1 R_2$, and $V_0 =$ constant, Eq. (9a) can be rewritten:

$$K_H = \left|\alpha\frac{1}{R_2}\frac{\tan(\beta\pi a_1)}{\beta\pi a_1}\frac{a_1}{\pi b_2}\int_0^{\pi}\frac{e^{-j\beta R_d(\varphi)}}{R_d(\varphi)}\cos(\varphi)d\varphi\right| \quad (23)$$

R_d is defined by Eq. (18b). Equation (23) can also be expressed logarithmically

$$k_H = 20\log(K_H) \quad \text{in} \quad \mathrm{dB}\left(\frac{\mathrm{A}}{\mathrm{m}}\frac{1}{\mathrm{V}}\right)$$

Equation (23) reduces the calibration of the loop to an accurate measurement of attenuation α for each frequency. The other terms of Eq. (23) can be calculated depending on the geometrical configuration of the calibration setup at the working frequency band of the measuring loop. The calibration uncertainties are also calculable with the given expressions. The uncertainty of the separation distance d between two loops must be taken into consideration as well. At a separation distance $d < r_1$ the change of the magnetic field is high.

For a calibration setup the separation distance d can be defined as small as possible. However, the effect of the mutual impedance must be taken into account in the calibration process and a condition to define the separation distance d must be given (Fig. 20). If the second loop is open circuited, that is the current $I_2 = 0$, the current I_1 is defined only from the impedances of the transmitting loop. In the case of a short-circuited second loop, I_2 is maximum and the value of I_1 will change depending on the supply circuit and loading of the transmitting loop. A current ratio q between these two cases can be defined as the condition of the separation distance d between the two loops.

It is assumed that the generator voltage V_0 is constant. The measuring loop **L2** is terminated by Z_L. For $Z_L = 0$ and

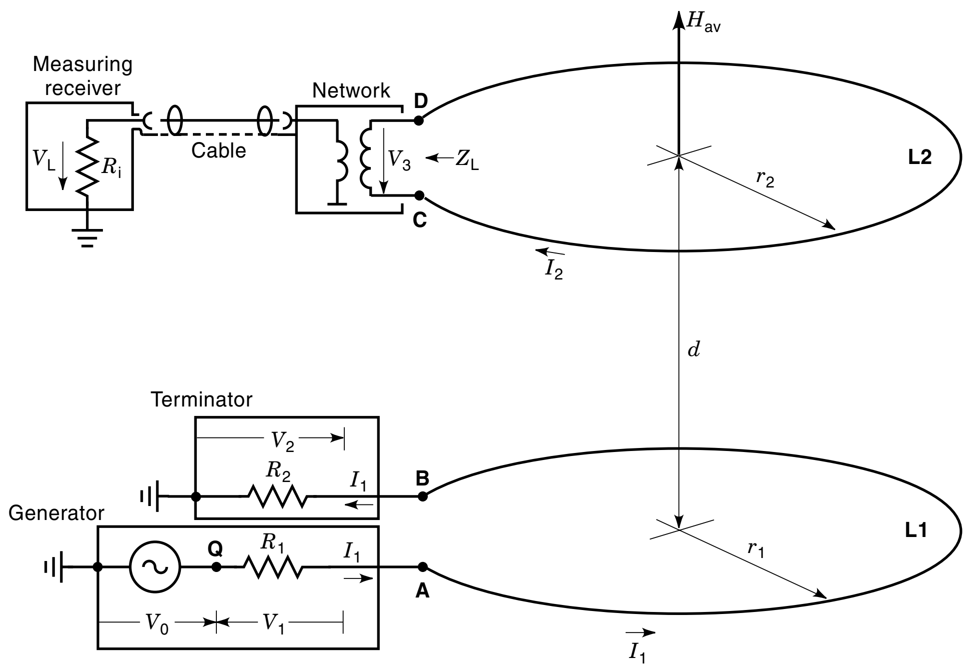

Figure 20. Calibration setup for circular loop antennas.

$V_{CD} = 0$, one obtains the current I_1 in the transmitting loop as

$$I_{1(Z_L=0)} = \frac{V_0}{R_1 + R_2 + Z_{AB} - \dfrac{Z_{12}^2}{Z_{CD}}} \tag{24a}$$

and for $Z_L = \infty$, i.e. $I_2 = 0$

$$I_{1(Z_L=\infty)} = \frac{V_0}{R_1 + R_2 + Z_{AB}} \tag{24b}$$

The ratio of Eq. (24a) to Eq. (24b) is

$$q \equiv \left| \frac{I_{1(Z_L=0)}}{I_{1(Z_L=\infty)}} \right| = \left| \frac{R_1 + R_2 + Z_{AB}}{R_1 + R_2 + Z_{AB}\left(1 - \dfrac{Z_{12}^2}{Z_{AB}Z_{CD}}\right)} \right| \tag{25a}$$

here with the coupling factor $k = Z_{12}/\sqrt{Z_{AB}Z_{CD}}$ between two loops:

$$q = \left| \frac{R_1 + R_2 + Z_{AB}}{R_1 + R_2 + Z_{AB}(1 - k^2)} \right| \tag{25b}$$

where $R_1 = R_2 = 50\ \Omega$, Z_{AB}, Z_{CD}, and Z_{12} can be calculated from Eqs. (15) and (19). For greater accuracy one must try to keep the ratio q close to unity (e.g., $q = 1.001$).

The influence of the loading of the second loop on the transmitting loop can also be found experimentally. The change of the voltage V_2 at R_2 in Fig. 20 must be considerably small, e.g. <0.05 dB, while putting a short-circuited measuring loop at the chosen separation distance.

With the determining of K_H or k_H the loop can completely be calibrated up to its 50 Ω output. A network analyzer is usually used for the attenuation measurement instead of a discrete measurement at each frequency with signal generator and measuring receiver. A network analyzer can normalize the frequency characteristic of the transmit loop and gives a quick overview on measured attenuation for the frequency band.

BIBLIOGRAPHY

1. CISPR 16 Specification for radio disturbance and immunity measuring apparatus and methods—Part 1: Radio disturbance and immunity measuring apparatus (8.1993); Part 2: Methods of measurement of disturbances and immunity (11.1996).
2. CISPR 11/2nd edition 1990-09 and EN 55011:07.1992: Limits and methods of measurement of electromagnetic disturbance characteristics of industrial, scientific, and medical (ISM) radiofrequency equipment.
3. *IRPA Guidelines on Protection against Non-Ionizing Radiation,* Oxford, UK: Pergamon Press, Inc., 1991.
4. ENV 50166 Part 1:1995—Human Exposure to electromagnetic fields—Low-frequency (0 Hz to 10 kHz) and Part 2:1995—Human exposure to electromagnetic fields—High frequency (10 kHz to 300 GHz).
5. VDE 0848 Part 4 A2:Draft 1992—Safety in electromagnetic fields. Limits for the protection of persons in the frequency range from 0 to 30 kHz and Part 2: Draft 1991—Safety in electromagnetic fields. Protection of persons in the frequency range from 30 kHz to 300 GHz.
6. IEEE standard C95.1-1991: IEEE Standard for Safety Levels with Respect to Human Exposure to Radio Frequency Electromagnetic Fields, 3 kHz to 300 GHz.
7. MIL-STD-461D, 11 January 1993: Requirements for the control of electromagnetic interference emissions and susceptibility, MIL-STD-462D, 11 January 1993: Measurement of electromagnetic interference characteristics, DOD, U.S.A.
8. VG 95373 Part 22, Cologne, Germany: Beuth Verlag, 1990.

9. J. R. Bergervoet and H. van Veen, A large loop antenna for magnetic field measurements, *Proc. Int. Symp. EMC,* 29–34, Zürich, 1989.
10. CISPR 15/5th edition 1996-03 and EN 55015:12.1993: Limits and methods of measurement of radio disturbance characteristics of electrical lighting and similar equipment.
11. Draft revision of IEC 945 (IEC 80/124/FDIS): Maritime navigation and radiocommunication equipment and systems—General requirements, methods of testing and required test results; identical requirements are given in Draft prETS 300 828/02.1997: EMC for radiotelephone transmitters and receivers for the maritime mobile service operating in the VHF bands, and Draft prETS 300 829:02.1997: EMC for Maritime mobile earth stations (MMES) operating in the 1,5/1,6 GHz bands; providing Low Bit Rate Data Communication (LBRDC) for the global distress and safety system (GMDSS).
12. U.S. FCC *Code of Federal Regulations* (CFR) 47 Part 18. Edition October 1, 1996.
13. J. E. Lenz, A review of magnetic sensors, *Proc. IEEE,* **78** (6): 973–989, 1990.
14. L. Rohde and F. Spies, Direkt zeigende Feldstärkemesser (Direct indicating field-strength meters), *Zeitschrift für technische Physik,* 10. Jahrg., Heft 11, 1938, pp. 439–444.
15. Data sheet edition 9.72 of Rohde & Schwarz Field-strength Meter HFH (0.1 to 30 MHz).
16. K. Danzeisen, Patentschrift DE 27 48 076 C2, 26.10.1977, Rohde & Schwarz GmbH & Co. KG, POB 801469, D-81614 München.
17. F. Demmel and A. Klein, Messung magnetischer Felder mit extrem hoher Dynamik im Bereich 100 Hz bis 30 MHz (Measurement of magnetic fields with an extremely high dynamic range in the frequency range 100 Hz to 30 MHz), *Proc. EMV '94,* Karlsruhe, 815–824, 1994.
18. CLC/TC111(Sec)61: Sept. 1995: Definitions and Methods of Measurement of Low Frequency Magnetic and Electric Fields with Particular Regard to Exposure of Human Beings (Draft 2: August 1995).
19. DKE 764/35-94: Entwurf DIN VDE 0848 Teil 1 “Sicherheit in elektrischen, magnetischen und elektromagnetischen Feldern; Meß- und Berechnungsverfahren” (Draft DIN VDE 0848 part 1 “Safety in electric, magnetic and electromagnetic fields; measurement and calculation methods”).
20. Recommendation ITU-R SM 378-5, *Field-strength measurements at monitoring stations,* SM Series Volume, ITU, Geneva 1994.
21. *Spectrum Monitoring Handbook,* ITU-R, Geneva 1995.
22. J. J. Goedbloed, “Magnetic field measurements in the frequency range 9 kHz to 30 MHz” EMC91, ERA Conference, Heathrow, UK: Feb. 1991.
23. F. M. Greene, The near-zone magnetic field of a small circular-loop antenna, *J. Res. Nat. Bur. Stand., Eng. and Inst.,* **71C** (4): 319–326, 1967.
24. A. Aykan, “Calibration of Circular Loop Antennas” to be published.
25. S. A. Schelkunoff, *Electromagnetic Waves,* New York: Van Nostrand, 1943.
26. J. Kaiser et al., Feldstärkeumrechnung von 30 m auf kürzere Messentfernungen (Conversion of field strength from 30 m to shorter distances), **110**: 820–825, 1989.

AYDIN AYKAN
MANFRED STECHER
Rohde & Schwarz GmbH & Co.KG

MAGNETIC FIELD MEASUREMENT. See ELECTROMAGNETIC FIELD MEASUREMENT.

MAGNETIC FIELD TRANSDUCER. See HALL EFFECT TRANSDUCERS.